Numerical Weather Prediction

Modelling the diurnal thermocline for daytime bulk SST from AATSR

Forecasting Research Technical Report No. 418

Lisa A. Horrocks, Andrew R. Harris[1], and Roger W. Saunders

at NOAA/NESDIS/ORA & University of Maryland

©Crown Copyright

Modelling the diurnal thermocline for daytime bulk SST from AATSR

by Lisa A. Horrocks, Andrew R. Harris, and Roger W. Saunders

Forecasting Research Technical Report Number 418

Version	Date	Comment	Amended by
1.0	16/07/2003	First draft for comment from coauthors	LAH
1.1	17/07/2003	More detail about quality of air-sea fluxes	LAH
1.2	13/08/2003	Addressed comments from R.Saunders on v1.0	LAH
1.3	15/10/2003	Addressed comments from J. Eyre on v1.2	LAH
1.4	15/10/2003	Approved as Technical Report by J. Eyre / R. Saunders	
1.5	22/12/2015	Corrupt equations were replaced	RWS

Abstract

Diurnal warming of the ocean's surface layers results in vertical temperature gradients in SST, and can cause significant (up to ~3 K) biases between satellite-derived measurements of the skin SST and in situ sampled bulk SST. In order to estimate a bulk SST from daytime retrievals of SST from AATSR data, it is important to assess the extent to which such a shallow diurnal thermocline might affect any given observation. We have investigated the performance of two published physically-based models in simulating diurnal thermoclines and a third, regression-based scheme. One of the physical models provided realistic simulations across most heat flux and wind speed ranges. This model was used in conjunction with heat flux and wind speed data from the Met Office NWP model in several case studies for validation against AVHRR-derived estimates of diurnal warming in the Mediterranean. Discrepancies between model predictions and the observations of diurnal warming were largely due to errors in the heat flux or wind data. Models to predict diurnal thermoclines have been integrated into a near-real time processing scheme for AATSR SSTs so that potentially affected data may be identified. The application of our favoured model provides realistic results, although accurate validation of these results is not possible. Screening of AATSR observations potentially affected by diurnal thermoclines resulted in a marginal improvement in bias and standard deviation of AATSR SSTs compared to collocated measurements from buoys. Given the uncertainties associated with NWP model surface flux data, the use of computationally expensive physical models in near-real time processing could be excessive, and a simpler scheme, tuned appropriately, may be the best pragmatic solution in this context.

1. Introduction

Infrared instruments are sensitive to the skin temperature. In situ sensors (buoys, ships) sample SST below the skin, at 1-m for buoys or more than 5-m on some ships. Discrepancies between these temperature measurements arise as a result of vertical gradients maintained in surface layers. Two main physical processes cause temperature gradients. The skin effect operates across the boundary layer at ocean surface and causes skin SST to be cooler than the SST immediately below the skin (subskin SST). This can be modelled accurately by relatively simple models, driven by heat flux and momentum flux data at to or close to the observation time (Horrocks et al. 2003a). Typical skin–subskin SST differences are ~–0.2 K, although when wind speeds are low the SST difference can be as much as ~–0.6 K.

The second process for consideration is that of shallow diurnal warming. Under clear skies, solar radiation is absorbed into surface waters (~30% of the total incident short-wave energy is absorbed in the top 2 cm); if there is sufficient wind-mixing energy, this absorbed energy is transported down, and the surface layer remains well-mixed. If wind speeds are very low, however, there is insufficient turbulent energy to dissipate the surface heating, the heated layer becomes buoyant, and thermal stratification, a diurnal thermocline, develops. Figure 1 shows a time series of skin and bulk SST data from a cruise. Both processes of the skin effect and diurnal thermocline are illustrated. While a diurnal thermocline is set up only twice during the time series in Figure 1, the skin–bulk SST difference when it occurs is up to 1.5 K. In fact shallow diurnal warming has been known to cause skin–bulk differences of more than 3 K in some cases (e.g., Fairall et al. 1996, Webster et al. 1996).

Shallow temperature gradients set up during diurnal warming can cause significant discrepancies between satellite (skin) and in situ SST measurements. In order to take advantage of the proliferation of satellite SST data over the past decades for climate monitoring, it is essential that the satellite measurements can be compared with historical SST records, which are invariably bulk measurements. In this context, and at the scale of accuracy required for climate research, skin–bulk differences caused by diurnal warming (and the cool skin effect) are not negligible. Furthermore, within satellite datasets themselves, it is important to understand (and possibly remove) diurnal biases: where shallow diurnal heating occurs, a daytime skin SST is temporarily elevated with respect to the skin SST at night. The extent to which diurnal warming affects global SST data has only recently been identified (e.g., Stuart-Menteth et al. 2003). Figure 2 shows a monthly mean of the SST difference computed from consecutive night and day overpasses from AVHRR during January 1989 (Stuart-Menteth, pers. com.). Large parts of the southern (summer) hemisphere, away from the high wind belts, show significant diurnal warming. The pattern is reversed for northern hemisphere summer. Similar patterns of diurnal warming have recently been identified in microwave SST data (Gentemann et al. 2003).

The infrared Along-Track Scanning Radiometer (ATSR) instruments have been designed to provide SST to accuracies of 0.3 K, with less than 0.1 K drift per decade, as required for use in climate change detection. We have shown that errors on night time SSTs derived from ATSR data and corrected for the cool skin effect may be even less than this (~0.1 K, Horrocks et al. 2003b). While a conversion from skin SST to subskin SST can be accurately made, via a model for the skin effect, this provides an estimate of bulk SST (i.e. at nominal depth of ~1 m) only at night, or under cloudy or windy conditions during the day (see Profile 1 in Figure 3). If daytime conditions are calm and clear, then diurnal warming becomes important, and the subskin SST is no longer an accurate representation of the 1-m bulk SST (see Profile 2 in Figure 3). In these circumstances, we would ideally predict the temperature difference between subskin and 1-m, in order to derive the true bulk SST from the ATSR skin SST measurement. In this report, we consider how to approach this problem, we investigate some published models which can be applied to diurnal thermocline development, we provide limited validation of one of these models and show how it can be applied to (A)ATSR SST processing. Finally we make some recommendations for future work.

2. Approaches to the problem

We need to address the issue of diurnal thermoclines in a near-real time environment applicable to routine processing of AATSR data for bulk SSTs across the globe. The approach is therefore similar to that for the problem of the cool skin effect: we look to an appropriate model of the top layers of the ocean which can be forced with appropriate heat and momentum flux data. One added complexity in the consideration of diurnal thermoclines is that the response seen at a given time is

the integrated effect of the flux history experienced at that location. In the case of the skin effect, the heat capacity of the skin layer is almost nil, and so the response is practically instantaneous. For diurnal thermoclines, the history of fluxes from dawn to observation time will be required: since the primary energy source is insolation, and thermal structures are usually entirely eroded through overturning driven by surface cooling at night, it is only the current daily cycle which is relevant. For near-real time applications, it is likely that the only source of surface flux data will be analyses from NWP models, and so in this study we concentrate on them. However for localised validation studies, more detailed in situ flux measurements may be available.

It is useful to define the problem in a general way in order to identify the important processes. We follow a general description with some more detail on two alternative 1-D upper ocean models for which we have developed code to address the problem of diurnal thermoclines in (A)ATSR processing. We mention also a third approach involving regression schemes based on either observations or model results.

2.1 A general case

We want to describe the temperature difference between the subskin SST and the bulk SST at some depth, in terms of the heat and momentum fluxes in the surface waters. The (A)ATSR product in use is provided as 10 x 10 arcminute cells, and daytime overpasses are at ~1000h local time for AATSR (or ~1030h for ATSR-1/-2). Given a typical ocean current speed of ~0.1 m s^{-1}, advection distances between sunrise and observation time are ~1–2 km, and the impact of advection can therefore be ignored at the scale of the AATSR data. One-dimensional column models are thus appropriate to our problem, and it is only the vertical heat and transport processes in the top few metres of the ocean which are relevant.

Considering an ocean layer in a vertical column, the temperature rise in that layer is expressed simply as

$$\text{temperature rise} = \frac{\text{heat source in layer + heat input from layer above + heat input from layer below}}{\text{heat capacity of layer}},$$

where heat source, heat inputs and temperature rise may all be positive or negative. For layers below the topmost, the heat source comes only from absorption of solar radiation within the layer. In the top layer, solar absorption contributes to the heat source term, but so do boundary transfer processes of latent, sensible and longwave heat. To restate the problem in more detail, for a layer i at depth z_i and of thickness dz_i, the temperature change, ΔT, in that layer between time t and $t + \Delta t$ is given by

$$\Delta T = \Delta t \; K_{i,i+1}(T_i - T_{i+1}) + K_{i-1,i}(T_{i-1} - T_i) + Q_i \frac{dz_i}{\rho_i C_p} \qquad (1)$$

where $K_{i-1,i}$ and $K_{i,i+1}$ are heat transfer coefficients between layers $i-1$ and i, and i and $i+1$, respectively, Q_i is the heat source within layer i, ρ_i is the density of layer i, and C_p is the specific heat capacity of seawater.

The heat source within each layer can be determined from commonly available parameterisations for the absorption of solar radiation (e.g., Paulson and Simpson 1977, Simpson and Dickey 1981, Morel and Antoine 1994). Strong absorption of near-infrared radiation makes the source terms

largest in the top layers. Despite some compensatory cooling through heat exchange at the surface, the net result is a strong temperature rise in the upper layers, which become more buoyant than layers beneath, and stable stratification under conditions of high insolation.

Heat transfer between neighbouring layers occurs through several processes. Once temperature gradients have been set up, conductive and diffusive transport will take place. However, because the molecular diffusivity of water is low ($\sim 10^{-7}$ $m^2 s^{-1}$), these processes are responsible for only minor redistribution of heat. Turbulent mixing processes are much more effective at transporting heat, and are the major method by which heat is redistributed through the column.

In order to describe the distribution of heat in the upper ocean, we turn to models of the ocean mixed layer (OML) incorporating heating and transport processes. Although the scale of the diurnal thermocline is one to two orders of magnitude smaller than that of the true OML, the physics in both cases is similar. Mixed-layer models fall into two categories: bulk and diffusion models. Bulk models describe the OML in an integral sense (e.g., Kraus and Turner 1967). Governing equations are integrated over the OML so that the heat and momentum balance of the whole layer under the action of fluxes at the ocean surface is considered. The increase or decrease in thickness of the mixed layer at the ocean surface must be parameterised in terms of surface fluxes, using either properties of turbulence in mixed layers, or observational evidence, but these parameterisations are far from universal. Price et al (1986) developed an alternative bulk model, dependent on the generation of shear instability at the base of the mixed layer. They also included parameterisations to account for the influence of stabilising (and destabilising) buoyancy fluxes at the surface, and achieved excellent model agreement with observations of diurnal mixed layers.

In contrast, diffusion models vertically resolve the OML and attempt to parameterise turbulent mixing and diffusion directly. This parameterisation can come from theoretical or observational knowledge of surface layers, resulting in empirical or semi-empirical formulations for turbulent diffusion (e.g., Large et al. 1994). This approach depends upon Monin-Obukhov similarity relations, with additional equations for the influence of surface buoyancy fluxes on mixed-layer depth. Alternatively, the parameterisation can come from actual modelling of turbulence quantities, appealing to turbulence closure at the second or third order (e.g., Mellor and Yamada 1982, Kantha and Clayson 1994). In this case, models are potentially "universal" and applicable to a variety of geophysical mixed layers (although model constants are defined empirically, they are essentially nontunable from one case to another). At its simplest, this parameterisation can consist of one equation for the conservation of turbulent kinetic energy, and a set of algebraic formulae for turbulence second-order quantities. However, as may be expected, diffusion models are generally much more computationally expensive than bulk schemes.

2.2 Kraus-Turner model

The model of Kraus and Turner (1967), hereafter "KT", addresses the problem in terms of energy budgets. The temperature profile is initially isothermal. At each timestep, heat is introduced through solar absorption causing a change in the temperature profile. Following this, for a heated layer *i* to be mixed with the cooler one beneath it, work must be done to offset the buoyancy caused by temperature rise. The energy for this work is derived from wind-mixing energy imparted to the topmost layer by wind stress. Heated layers can be mixed downwards so long as there is enough wind-mixing energy available to overcome the opposing buoyancy in the layer. Surface cooling provides a source of negative buoyancy which is augmented by an increase in salinity (and hence density) due to evaporation: the top layer can thus become unstable relative to the layer beneath. Mixing processes are assumed to be instantaneous. The result is a uniform raised temperature

distribution in the uppermost layers down to the depth at which all available wind-mixing energy has been exhausted, with any deeper layers retaining the temperature obtained through solar absorption alone. For subsequent timesteps, the initial temperature profile is that calculated at the end of the preceding timestep.

Implementation of the KT model is straightforward. The primary quantity governing vertical mixing is the energy required to mix the next layer with the layers above, and the heat transfer coefficients identified in Eq. (1) are irrelevant because there is no time dependence of mixing. The potential energy required for mixing, *dP*, depends upon the difference in density between adjacent layers, and the layer thickness, as shown in Equation (2), where symbols have the same meanings as before, and *g* is the acceleration due to gravity.

$$dP = \frac{g}{2}(\rho_{i+1} - \rho_i) z_i dz_{i+1} \qquad (2)$$

Density is a function of temperature and salinity and parameterised via a linear "equation of state" based on mean values for the water column under consideration.

The KT model has been used to model the vertical transport of heat in the ocean for many years, particularly at climate resolution where the exact nature of turbulent transport at short temporal and spatial scales is unimportant. The Met Office Unified Model includes a KT scheme for the OML: we have adapted a one-dimensional version of this scheme to model the diurnal thermocline.

2.3 Kantha-Clayson model

The model of Kantha and Clayson (1994), hereafter "KC", is regarded as one of the best turbulence models for geophysical boundary layers in recent years. It was developed from second-order turbulence closure models originally formulated by Mellor and Yamada (e. g., 1982). Treatment of shear instability induced mixing in the strongly stratified region below the mixed layer follows the method of Large et al. (1994).

The KC model has been validated at different timescales and in a number of locations (KC), and importantly, it has been used to model the diurnal thermocline (Wick 1995, Webster et al 1996). We have taken the form of the model developed by G. Wick for the diurnal scenario, and developed it further so that KC and KT models may be operated interchangeably within the same framework (Horrocks et al. 2002).

Differential equations for the evolution of several geophysical quantities (e.g., velocity, temperature, salinity) with time are set up. For example, the model equation for the evolution of temperature, *T*, with time, *t*, in a single layer is

$$\frac{\partial T}{\partial t} = \frac{\partial}{\partial z}\left(\frac{\nu}{\sigma_P} + K_H\right)\frac{\partial T}{\partial z} + \frac{Q}{\rho C_p} \qquad (3)$$

where ν is molecular viscosity, σ_P is the molecular Prandtl number, K_H is the turbulent diffusion, and all other symbols carry the same meanings as before. In effect, this is a differential form of Eq. (1), with the mixing (i.e., heat transfer between layers) coefficient, *K*, in Eq. (1) here defined as the sum of molecular (ν/σ_P) and turbulent (K_H) diffusivities. In practice, the model adopts a value for oceanic background diffusion, K_{HB}, due to eddy production and mean current shear in place of the molecular diffusivity (ν/σ_P).

The turbulent diffusivity, K_H, is modelled in terms of a stability parameter, S_H, as

$$K_H = q\ell S_H \tag{4}$$

where q^2 is twice the turbulent kinetic energy (TKE) and ℓ is the turbulent length scale. S_H depends upon buoyancy production, TKE production and ℓ, and is parametrised following Equation (5).

$$S_H = \frac{A_2\left(1-\frac{6A_1}{B_1}\right)}{1-3A_2(B_2+6A_1)G_H} \tag{5}$$

A_1, B_1, etc are constants which have been derived by a number of authors from large eddy simulations and observations and are effectively universal. G_H is a buoyancy parameter, defined as

$$G_H = \frac{\ell^2}{q^2}\,\beta g \frac{T}{z} \tag{6}$$

where β is the expansion coefficient and all other symbols carry their previous meanings. The end result of Eq. (3) to (6) is to describe the ability of turbulence to diffuse heat as dependent upon buoyancy production. This is similar to the energy balance envisaged in KT, above, between available wind-mixing energy and opposing buoyancy due to thermal expansion.

Determination of the production of TKE involves all the prognostic equations of the mixed layer model. Turbulence is modelled in three dimensions to incorporate shear and downward transport, and depends upon eddy viscosity (K_M), and thermal- and salinity-induced buoyancy. The reader is referred to KC for full details of equations.

Following initial tests in simulation and against in situ SST profiles (not presented here), values for the background molecular mixing terms (K_{HB} and K_{MB}) were adjusted to be more appropriate for the scale of the diurnal thermocline. Originally, these values had been determined for the full OML.

When implemented computationally, the solution for the current timestep depends upon the solution for the previous timestep. To overcome numerical instability, a combination of forward-, central-, and backward-differencing is used: in conjunction with smoothing factors, this reduces model sensitivity to small fluctuations. We have included a spin-up of 5 timesteps to avoid sharp temperature fluctuations in the upper layers on initialisation of the model.

2.4 Regression schemes

A third option for predicting diurnal thermocline temperature differences is to use regression schemes based either on observations or on results from models such as those described above. For the latter, the approach is still based on one of the two physical descriptions, bulk or diffusion, but more direct links between forcing conditions and resultant temperature differences are determined.

Kawai and Kawamura (2002) used meteorological data from buoys and satellite-derived solar radiation to evaluate a one-dimensional numerical model for the amplitude of the diurnal SST variation ($\mathbf{\Delta}SST_{max}$, defined by them as the difference between the maximum after 0900 LST and the minimum before 0900 LST, for either skin SST or SST at 1-m depth). In order to avoid any complication from heat advection in SST variations observed from buoys, they used results from their model to determine a more simple regression equation linking the amplitude of the diurnal signal with peak solar radiation (PS) and wind speed (u). Results showed a linear relation of $\mathbf{\Delta}SST_{max}$ with $\ln(u)$ and a linear relation of $\mathbf{\Delta}SST_{max}$ with PS^2. Webster et al. (1996) had proposed a similar regression for the diurnal amplitude of skin SST, but they also included a dependence on precipitation. Kawai and Kawamura neglected any dependence on precipitation because of the difficulty of obtaining precipitation data over a wide region. For application to infrared satellite data, any dependence on precipitation is irrelevant as observations are only available in cloud free conditions. Both sets of authors noted a change in regime at wind speeds of 2 or 2.5 ms^{-1} and supply alternative values for coefficients in their regression equations above and below this threshold. Kawai and Kawamura later modified their empirical formula to include daily mean latent heat flux (H_l), and they replaced the peak solar radiation with a daily mean solar radiation (MS) to match the use of mean latent heat flux (A. Stuart-Menteth, pers. com.). The final regression equation is given in Eq. (7), with values for the coefficients a to e in Table 1.

$$\Delta SST_{max} = a(MS - H_i + e)^2 + b\ln(u) + c(MS - H_i + e)^2\ln(u) + d \qquad (7)$$

Table 1. Coefficients for the modified version of the regression equation from Kawai and Kawamura (2002).

	for diurnal signal at skin		for diurnal signal at 1-m depth	
	u > 2.5 m s^{-1}	u ≤ 2.5 m s^{-1}	u > 2.5 m s^{-1}	u ≤ 2.5 m s^{-1}
a	1.0418 x 10^{-5}	2.5938 x 10^{-5}	7.8280 x 10^{-6}	9.1299 x 10^{-6}
b	9.4600 x 10^{-2}	3.2704	1.3810 x 10^{-1}	1.0346
c	-3.8472 x 10^{-6}	-2.0785 x 10^{-5}	-2.8906 x 10^{-6}	-4.3115 x 10^{-6}
d	-2.5618 x 10^{-1}	-3.1661	-3.7399 x 10^{-1}	-1.1954
e	300.0	300.0	300.0	300.0

Gentemann et al. (2003) used satellite derived observations of infrared and microwave SSTs and wind speed, combined with a weekly bulk SST analysis and calculations of daily mean clear sky insolation to define an empirical model for diurnal SST warming. The data showed a linear dependence of the difference between infrared skin SST and bulk SST $\mathbf{\Delta}(T_{s\text{-}b})$ on insolation (Q), an exponential dependence of $\mathbf{\Delta}T_{s\text{-}b}$ on wind speed (u), and a local-time dependence of $\mathbf{\Delta}T_{s\text{-}b}$ described by a Fourier series. The model equation derived by non-linear least squares regression is given below

$$\Delta T_{s-b}(t, Q, u) = 0.344\, f(t)(Q - Q_0) - 1.444 \times 10^{-3}(Q - Q_0)^2 e^{-0.29u} \qquad (8)$$

The time-dependence term, $f(t)$ is given as a five-term Fourier series, for which the reader should refer to Gentemann et al. Q_o is a minimum value of solar insolation, set to 24 Wm^{-2}. No diurnal signal was discernible when solar heating was weak, and so the model set to zero when Q is less than Q_o.

The advantage of determining a simple regression is that computation time is minimal. However, it is unlikely that a regression equation can capture the details of a more complex model response to varying fluxes. If the flux data available to force a more complex model are of coarse resolution in time and/or space, this may not be such a disadvantage. The appropriateness of the regression is also dependent on capturing the full range of possibilities in the training data: if new observations fall outside this range, then the regression equation will not necessarily remain relevant.

3 Model implementation and simulations

3.1 Implementation of vertical mixing models

A generic interface to a choice of shallow diurnal warming models is used to set up the flux histories relevant to the observation under consideration. The method for the full models is described below; for the regression scheme appropriate flux averages are used in independent calculations for skin and 1-m levels.

Since we are interested in the temperature structure of the uppermost ocean, we have implemented a depth-dependent layer thickness, starting at 2 cm for the topmost layer and increasing exponentially to ~60 cm at the 60th layer. A depth of ~10 m is covered in this way and coupled to two deeper layers at 51 and 100 m to provide a sink for downwardly-mixed energy.

A time-history of surface fluxes is available at 6-hourly intervals from the Met Office NWP analysis. For a high resolution model of the near-surface (KC, KT), the solar flux, at least, needs to be converted to a finer time resolution. This is achieved by first calculating the integral over a day from the available 6-hourly averages (or instantaneous values), and then solving the integral equation for the time of year and latitude-longitude location of the observation, to find an equivalent peak insolation, $S_{\max}$:

$$S_{\max} = \frac{\pi \int Q_{sol}\, dt}{H \sin\phi \sin\delta + \cos\phi \cos\delta \sin H}, \qquad (9)$$

where Q_{sol} is the 6-hour mean solar flux, ϕ is latitude, δ is solar inclination (i.e., the latitude at which the sun is directly overhead, a function of day of year only), and H is the half-day (sunrise to noon) in radians, calculated as

$$H = \cos^{-1}\left(-\tan\phi \tan\delta\right). \qquad (10)$$

$S_{\max}$ is the insolation at local noon required to produce the daily total solar flux, assuming a smooth variation with time, ignoring any variation in cloud cover during the day. The solar flux is derived from this curve at 10-minute timesteps and the model is run from sunrise to the time of the daylight AATSR overpass. Other fluxes required by the models (latent heat, total non-solar radiation, sensible heat, wind-mixing energy) are retained at 6-hour resolution, each timestep set to the appropriate average value. Precipitation effects are not explicitly included in the evaluation of surface fluxes since AATSR data are for clear skies only.

For solar absorption, two- or three-band parameterisations (Paulson and Simpson 1977, Morel and Antoine 1994) are not adequate given the accuracy required in the skin–bulk SST context: they underestimate near-surface absorption so that derived heating rates would be questionable. Instead, we have adopted the nine band exponent parameterisation of Simpson and Dickey (1981). The heat source term in each layer is calculated as the difference between the flux entering the top and the flux leaving the base; this latter becomes the flux to enter the top of the layer below. For layer i, this can be expressed as

$$Q_i = I_o \sum_{j=1}^{9} \alpha_j \left(e^{z_i/\eta_j} - e^{z_{i-1}/\eta_j}\right) \qquad (11)$$

where z_i is the layer depth, I_o is the insolation at the surface (less that reflected) and α_j, η_j are the Planck weighting and e-folding depth, respectively, for band j. The sum total of α_j is 1. In practice,

the transmittances are calculated in sequence so that only nine exponentials are evaluated for each model layer. No attempt is made to compensate for differential heating within each layer since the layers are thin, especially at the top where the absorption profile is steepest.

The temperature profile is initialised to the surface SST value at the start of each run, and the default salinity is 35 kg m^{-3}, which is subsequently modified within the models by evaporation.

To investigate the models, we have run simulations using fixed values of fluxes, wind speeds and peak solar radiation, and examined the response of the models as a function of time of day and changing wind speed.

3.2 Simulation results

In Figure 4, the evolution of the diurnal thermocline in the top 6 m of the ocean is shown for idealised simulations with both KC and KT models. For these simulations, a peak solar radiation of 1000 W m^{-2} was assumed, with maximum at 1200 h from a sunrise at 0600 h. Latent heat flux was fixed at 75 W m^{-2} and the net non-solar fluxes (latent heat + sensible heat - downwelling longwave radiation) were 150 W m^{-2}. The wind speed was assumed constant at ~2.0 m s^{-1}, but the effect of different wind speeds is examined in Figure 5.

For both models, Figure 4 indicates that maximum surface temperature excursions occur well after the peak insolation, sometime around 1500 h in our simulation. The delay arises because it is only after about 1500 h that there is sufficient residual wind mixing energy to dissipate heat downwards. Before this time, all the wind-mixing energy is used up in overcoming buoyancy generated either in that timestep or residual from the timestep before. Given that (A)ATSR daylight overpass times are 1000-1030 h local, the surface diurnal warming expected from these simulations would be ~0.5 K from KC model, and possibly slightly more from KT. Satellite instruments with afternoon overpasses (e.g., AVHRR on board NOAA platforms) will be more strongly affected. By 1600 h, the KC model predicts the onset of erosion of the maximum diurnal thermocline obtained earlier in the day. The KT model takes much longer to erode the more extreme (and unrealistic) surface temperature predicted in this simulation.

Differences between the models are highlighted in the shape of the profiles in Figure 4. As the KT model is constrained by energy conservation in each layer, the shallowest layers always remain completely mixed, giving an isothermal gradient down to the depth at which mixing energy is used up. Consequently, at very low wind speeds, the KT predicts shallow completely-mixed layers at unrealistic high temperatures with extreme temperature gradients below (e.g., for a wind speed of 1.0 ms^{-1} in Figure 5, the top 5 cm reached 35 °C, falling off to 25 °C immediately beneath) – in reality these are unlikely to be sustained due to the contribution of diffusive mixing. They are sustained in the KT model because this does not include a diffusion term. In the KC model, temperature gradients, even at low wind speeds, remain much more realistic because diffusion is included explicitly. In an independent evaluation against in situ profiler data, the KT model was consistently found to overpredict the magnitude of diurnal thermoclines, particularly when the wind-mixing energy was low (A. Harris, pers. com.).

In general, the KT model appears to be a reasonable indicator of when diurnal thermoclines should be expected, but it is inadequate to predict the magnitude. The main limitation of the KT model is that it is entirely reliant on mechanical and buoyancy-driven mixing. In the absence of either mixing mechanism (i.e., under strong solar heating and low windspeed) heat simply builds up in the top layer and there is no mechanism by which it may be drawn downward (either by diffusion or even conduction). This leads to a very shallow stratified layer and consequently the unrealistic diurnal excursion which we have observed in simulation. For applications in which it is preferable to model the magnitude of the diurnal thermocline accurately, the KC model is far more promising, on the basis of simulations, than the KT, and we concentrate hereafter on an evaluation of the KC model.

The combined impact of wind speed and peak solar radiation on simulations of the KC model is shown in Figure 6. If the peak solar radiation is reduced (to simulate locations at higher latitudes or partially cloudy days) the amount of diurnal warming is strongly affected: there is insignificant surface warming if peak solar radiation is less than ~500 Wm^{-2}. If wind speeds are higher than ~4.0 ms^{-1}, as seen also in Figure 5, the available wind-mixing energy is enough to mix down most of the buoyancy from surface heating, preventing development of strong surface temperature excursions. Changes to the fixed values used for the other fluxes (latent and sensible heats and longwave IR) affected the magnitude of the temperature excursions but not the overall pattern of the model response. As the net heat flux out of the ocean increased, the strength of the diurnal thermocline for a given peak solar radiation and wind speed decreased.

For wind speeds greater than ~7 ms^{-1}, which is the mean ocean wind speed, Figure 5 shows that neither model predicts any significant thermal stratification. The value of 1000 Wm^{-2} used in these simulations for peak insolation is a realistic maximum for this parameter, and Figure 6 showed that surface heating was much reduced at lower values. So diurnal thermoclines are expected to show geographical preferences for areas where winds are light and persistent strong insolation is common. This is borne out in the global distribution in Figure 1, and elsewhere (Stuart-Menteth et al. 2003), and by regular observations of large diurnal thermoclines in areas like the West Pacific warm pool (e.g., Webster et al. 1996). Changes in atmospheric conditions (e.g., cloud cover and therefore insolation during ENSO cycles) can affect the strength of diurnal signals and potentially cause apparent bias in the SST record not associated with real change in ocean surface temperature. Note also from the model profiles in Figures 4 and 5 that under favourable conditions, diurnal signals in SST may persist at the depths of in situ sensors on buoys (~1 m) or ships (~3–7 m). This has some implications for the historical climatological SST record in which diurnal signals in SST have been little considered.

Figure 7 shows temperature profiles at 1600h predicted by the KC model (similar to Figure 5), but with maximum diurnal temperature excursions predicted using the regression scheme of Kawai and Kawamura (2002) also shown, for comparison. For this scheme, the simulated insolation curve was averaged to provide a daily mean solar flux, and other heat fluxes were the same as before. Kawai and Kawamura (2002) provide coefficients for computing maximum diurnal warming at the surface and at 1-m depth: results from both calculations are shown in Figure 7. For all wind speeds, the Kawai-Kawamura scheme predicts a larger temperature excursion than the KC model. In application of their regression equation to real data in the W. Pacific, Kawai and Kawamura found that predicted diurnal SST excursions were often more than ~3 K, which seems high compared to most observations of diurnal warming. However, with some tuning of the Kawai-Kawamura coefficients, it may be possible to develop this computationally cheap scheme to replicate the KC model quite closely.

4 Validation against AVHRR data

4.1 Data and methods

The AVHRR is a single-view instrument, flown on board NOAA polar-orbiting satellites, and uses infrared channels at ~11 and 12 microns for SST measurement (similar to the (A)ATSR 2-channel retrieval). Comparisons of SST retrieved at night and during the day from AVHRR has been used to identify the extent of diurnal warming across the globe (Stuart-Menteth et al. 2003, Gentemann et al. 2003). Two features of AVHRR make it more suitable for this purpose than AATSR: first, it has a wider swath (2000 km as opposed to ~500 km on AATSR) which means that there is significant overlap of consecutive night and daytime overpasses. Secondly, for the Pathfinder reprocessing program, the same algorithm was used for both night and day data and so SST retrievals are directly comparable. The difference between daytime SST and the previous night time SST recorded in the same location provides a direct measurement of diurnal warming. Other work has used this information to assess a global climatology of shallow diurnal warming, both the phase and amplitude of the signal, and the impact of daylight satellite overpass time (Stuart-Menteth et al.). We have used these observations of diurnal warming in a restricted area to evaluate the KC model as it might be configured in an operational SST processing system.

The Mediterranean Sea was chosen as the study area because it is often cloud-free and known to be frequently affected by diurnal thermoclines during summer months. Additionally, this region should be accurately represented in NWP models, due to good availability of observations: this is crucial to the validation of the KC model which is driven by heat flux and wind speed fields from NWP analyses. July 1997 was chosen as the study month because NOAA-14 AVHRR daylight overpass times were 1400–1430 h local time during that period, and should therefore monitor close to the maximum of the diurnal cycle (see Figure 4).

The AVHRR SST data were from the Pathfinder v4.1 dataset, at 18 km resolution, and only those observations identified as cloud-free were used. The observed diurnal SST difference was calculated following Stuart-Menteth et al., defined as the difference between collocated daytime and night time SSTs. To increase the number of day-night matchups, daytime SSTs were coupled with the preceding night time SST, or, if this was unavailable, with the night time SST from two nights' previous. Note that the MCSST algorithm used to determine the SSTs in the Pathfinder dataset is essentially based on regression of TOA brightness temperature values against quality-controlled buoy observations of SST. The AVHRR SSTs may not fully represent the skin SST (as with (A)ATSR), but instead some estimate of bulk SST (assuming a constant offset between buoy SST and the temperature of the radiative skin). In the KC model, it is difficult to know exactly to which level in the temperature profile the AVHRR-derived SST should correspond. Because the diurnal signal seen by the satellite instrument must be determined by fluctuations in the skin temperature, we have compared the observed diurnal SST difference with model predictions of SST change in the surface layer.

For each AVHRR measurement of diurnal warming, heat flux and wind speed “histories” were determined from Met Office NWP model analyses of surface fields, as described in section 3.1. As indicated there, the flux data were available every 6 hours, and so an estimate of the solar cycle was obtained by extrapolation. The model temperature profile was initialised to the night time SST in the AVHRR dataset and the KC model was run from local dawn through to the daylight satellite overpass time. The predicted change in SST was then compared to the change in SST calculated from the AVHRR observations.

4.2 Selected case studies

The performance of the KC model compared to the AVHRR observations was studied day by day throughout July 1997. Some representative case studies are described here. Figure 8 shows the measured and predicted day–night SST difference for 14 July. There was a clear signal of diurnal thermocline development in the observations with day–night SST differences of up 3 K in a band south and north of Sicily. Gaps in data coverage occur where cloud was detected or where there was no overlap between daytime and nightime satellite overpasses. The observations also showed areas where the daytime SST was a few tenths of Kelvin cooler than the corresponding night time SST. Discrepancies at this level could be explained as uncertainty in the AVHRR retrievals, as inadequate daytime cloud detection, or by advection of cooler surface waters during the day. The KC model prediction of diurnal warming shows some skill on this day: the magnitude and location of the warm daytime SSTs are both reasonable. An implication of this is that on this day, the NWP analysis flux data used to drive the KC model must have been a good representation of the real conditions.

Figure 9 shows measured and predicted day–night SST differences for 10 July. In this case, the observations show strong diurnal warming in the central Mediterranean, while the model predicts weaker diurnal warming located much closer to southern Italy. This error in prediction is caused by errors in either the solar flux data or the wind speed data used in the model. The solar flux data in Figure 10 show no evidence for wrongly placed cloud to prevent the right conditions for diurnal warming. In Figure 11, we compare satellite observations of wind speed over the Mediterranean (from SSM/I, data available from www.remss.com) with the NWP wind analysis. While the observations reveal extremely low wind speed in exactly the area of diurnal warming from AVHRR, in the NWP field the area of very low wind is slightly misplaced to the west. The NWP analysis also fails to represent coastal effects: the observed wind off the coast of southern Italy is significantly stronger than in the analysis. So in this case, where clear conditions have been replicated in the solar fluxes, the accuracy of the wind data used in the model was crucial to the diurnal thermocline prediction. It should be noted that wind speeds from SSM/I are now assimilated into the NWP model and so the NWP wind field should now be closer to the satellite observations than in 1997.

The alternative problem of correctly representing cloud is demonstrated by the case on 22 July. Figure 12 shows the measured and predicted day–night SST differences. A striking feature in the observations is the band of negative SST difference sweeping SE from Sicily, but there is only weak diurnal warming seen elsewhere. By contrast, the KC model predictions identify a centre of strong diurnal warming just east of Sicily. The negative day–night SST difference is the result of undetected daytime cloud. The corresponding daytime AVHRR imagery is shown in Figure 13: the thicker cloud in the western Mediterranean is obvious, but there is also evidence for thin cloud stretching SE from Sicily, and this has not been detected during the Pathfinder SST processing. The NWP 6-hour mean solar flux analysis is also shown in Figure 13: a band of cloud is predicted in the model, but it is further south than the cloud identified in the imagery. Two problems are highlighted here. Firstly, inadequate cloud detection in satellite SST processing can result in spurious observations passing through. Secondly, the NWP model does not always locate cloud accurately, and this results in severe errors in solar flux fields (and hence an incorrect prediction of diurnal warming in an area actually beneath cloud).

During the study month of July 1997, the problem of undetected cloud in the AVHRR data was common, and in about 40 % of cases the resulting pattern of day–night SST difference was either too bland or too cloud-contaminated to use for model validation. Out of the remaining cases, the

pattern of diurnal warming was well-predicted about 50 % of the time, at most. For the rest, the model either failed to predict strong diurnal warming, or predicted diurnal warming where the observations showed there was none. In all of these, the main cause of error was the accuracy of solar flux or wind speed data from the NWP analyses.

The KC-model has been shown to be a reliable predictor of diurnal warming, by comparison with AVHRR SST observations, so long as the flux data used to drive it are accurate. For the 14 July case study (Figure 8), we also used the Kawai-Kawamura scheme to predict the maximum diurnal excursion at the surface and at 1-m depth. As expected from our simulation results, the magnitude of warming predicted from this scheme was too high; the locations of diurnal thermoclines were successfully predicted, however, since these are controlled by the accuracy of the solar flux and wind fields, rather than the choice of model.

5 Application in near-real time (A)ATSR data processing

5.1 Method

The AATSR daylight overpass is at ~1000 h local time (~1030 h for ATSR-1 and -2). From simulation results, it is clear that any diurnal warming will not have attained its peak, but Figure 4 indicates that surface temperature excursions of ~0.5–1.0 K are quite possible. In terms of bulk SST processing, it is not the day–night surface temperature excursion that is important, but the temperature difference between surface (skin) as seen by AATSR and bulk (at say ~1 m for average buoys) that matters. In order for AATSR SST data to be compatible with the historical climate record of bulk SST, any temperature gradients between the depth of traditional in situ samplers and the skin must be accounted for, and the magnitude of diurnal thermoclines even at 1000 h are significant given the accuracy that SST records aspire to. If the shape of the temperature profiles simulated in Figure 4 are realistic, then temperature differences of ~0.5 K between skin and 1-m depth are possible by 1000 h. A number of recent studies have reported direct measurements of near-surface temperature gradients (e.g., Webster et al. 1996). A variety of profile shapes seems to occur in nature; some of these are similar to the idealised KC profiles in Figures 4 and 5.

Within the (A)ATSR SST processing scheme, the KC model is run for every daylight observation. Histories of flux and wind speed data are obtained from NWP analyses. The profile is initialised to the retrieved skin SST, and the model is run from local dawn through to the observation time. The final temperature profile is used to determine the predicted temperature difference between skin and 1-m depth. The observation is flagged if this difference is more than 0.2 K, which would be large enough to offset an average cool skin effect. Since NWP surface flux and wind fields are known to contain significant inaccuracies at times, we do not use the predicted temperature difference to convert the retrieved AATSR skin SST to a 1-m depth SST. Instead, we advise that data flagged as affected by diurnal warming should be excluded from assimilation into climatological records, or at least given very low weight.

5.2 Results from AATSR

Figure 14 shows results from two different months of AATSR SST processing. Simple monthly averages were generated on a 0.5° latitude/longitude grid and then further averaged to 1° resolution for plotting. The frequency plots in the top of Figure 14 show the number of times that the KC model predicted skin–1-m SST differences of more than 0.2 K as a percentage of the number of valid daylight SST retrievals in that grid box. The increase in diurnal warming in the N. Atlantic

and Mediterranean in N. Hemisphere summer can be seen by comparison of the June plot with April. During April, diurnal thermoclines were frequently predicted in the W. Pacific warm pool. The bottom half of Figure 14 shows the average predicted skin–1-m SST difference for all daylight AATSR observations. During April, the strongest diurnal warming is predicted in W. Pacific, but in June, diurnal signal is strongest in the Mediterranean. The strongest diurnal thermoclines in these figures are rarely more than 0.5 K, in keeping with our expectations from the simulations shown in Figure 4.

The distribution of KC model predictions in Figure 14 seems reasonable, but these results are difficult to validate, since day-night SST retrievals from AATSR cannot be directly compared (the narrower swath-width of AATSR relative to AVHRR results in little overlap between consecutive days and nights). Comparisons of these AATSR data with independent SST analyses could be used to see whether larger discrepancies are found where the strongest diurnal warming is predicted. However, uncertainty in SST analyses means that these comparisons are frequently dominated by errors from alternative sources, and any signal from diurnal warming is lost in noise. Figure 14 is similar to the pattern of diurnal warming seen in monthly climatologies from AVHRR observations (Stuart-Menteth et al. 2003). As the AVHRR diurnal warming climatology becomes available for 2003 (and NOAA-17 AVHRR has a local overpass time quite similar to AATSR - 1100h compared to 1000h), this may provide one means with which to judge the overall pattern of KC model predictions from AATSR processing.

We have attempted to use coincident buoy and AATSR observations (matchups) to demonstrate the advantage of screening out those observations with predicted diurnal thermoclines. The buoy matchup dataset covered the period 19 August 2002 to 31 May 2003, and was constructed following Candy and Horrocks (2002). The buoy and satellite observations of SST were constrained to be within 3 hours of each other. Out of 2112 daytime matchups, 40 were flagged with predicted diurnal thermoclines of more than 0.2 K. AATSR skin SST was retrieved using dual-view and 2-channels, and retrieval coefficients generated in May 2003 from simulations with the latest version of RAD7 radiative transfer model at Edinburgh University. The difference between AATSR skin SST and buoy "bulk" SST was determined for all of the daytime matchups and then again after rejecting the 40 flagged data.

Table 1. Statistics from matchup database calculations.

	AATSR–buoy SST difference		
	mean / K	S. D. / K	Number
Daytime matchups	0.178	0.591	2112
Daytime without thermoclines	0.168	0.579	2072
Night matchups	0.043	0.500	1736

Note: The AATSR SST retrievals are known to be biased warm by ~0.18 K.
Night time AATSR SSTs were 2-channel retrievals for comparability.

The mean and standard deviation of the SST difference were both reduced by 0.01 K when the thermocline-affected observations were omitted. The change in mean bias is statistically insignificant. However, the difference in *variance* when the flagged data were omitted, of ~0.014 K^2, implies that a source of random error of ~0.12 K has been removed. This is a marginally significant improvement at the level of accuracy we aim to achieve with (A)ATSR. At the very least, these results show that our diurnal thermocline model can identify some of the worst data. It should also be noted that a large proportion of the variance in AATSR-buoy SST difference may come from uncertainty on the buoy measurement, and, particularly for daytime data, the potential spatial and temporal variability of observations collocated within 10 arcminutes and 3 hours. Were

we to constrain the matchup criteria further in the hope of reducing this potential variability, we would have far fewer data to work with.

6 Discussion and future work

Both the models and the regression scheme featured in this study have shown some skill in relating diurnal variation in SST with the forcing factors of insolation, net heat flux and wind speed. We have shown that these models can be successfully incorporated into satellite SST processing. The KC model provided more realistic SST variations (especially under extreme conditions) than the KT model because diffusive heat transfer was included explicitly. The KC model was also preferred to the Kawai-Kawamura regression scheme, which seemed to overestimate the magnitude of diurnal warming. Our limited validation showed that when the forcing data were accurate, the KC model provided excellent agreement with observations of diurnal warming, in both geographical extent and the magnitude of the SST change (e.g., Figure 8).

It is the quality of the forcing data which is crucial to the performance of any scheme to predict diurnal warming. For a global system operating in near-real time, the only source of flux data capable of providing "histories" for each observation is NWP model analyses. The Mediterranean validation indicated that 6-hour temporal averages for the flux data could be adequate, providing that they were accurate representations of the flux history, and were accurate spatially too. McCulloch and Hines (2003) showed that an NWP air-sea flux climatology, although balanced annually over the global oceans and for the Mediterranean basin alone, could nevertheless have biases of at least 30 Wm^{-2} in some regions: the N. Atlantic ocean heat loss was underestimated by this amount compared to in situ observations (following Isemer et al, 1989). The NWP model air-sea fluxes are dependent in part on semi-empirical bulk formulae to convert between meteorological variables and heat flux quantities. These formulae contain errors and Gleckler and Weare (1996) estimated that surface heat flux climatologies derived from ship observations via these methods could frequently have both systematic and random uncertainties approaching 30 Wm^{-2} (~10–20 %). We have also seen in the daily Mediterranean case studies that the location of clouds in NWP analyses may often be incorrect, and that the wind field itself may be spatially inaccurate. These errors in forcing data result in errors in diurnal thermocline model predictions.

For accurate SST datasets for climate studies, processes which cause biases between different SST data types (e.g., satellite and in situ) must be addressed. One approach, adopted by the GHRSST-Pilot Project , is to merge satellite and in situ SST measurements with models of the cool skin effect and the diurnal cycle. In this way analyses of SST fields at different depths can be produced, but it will be some while before this project completes. An alternative approach, taken by the Met Office, is to retrieve satellite skin SST accurately, and then to use physical models for the skin effect and diurnal thermocline to convert to an equivalent bulk SST, nominally at 1-m depth. This converted measurement can then be used directly in conjunction with in situ measurements (from buoys, ships etc) in climate SST analyses. While this conversion process is straightforward for night-time satellite data, with only the cool skin effect to consider (e.g., Horrocks et al. 2003a), this study has shown that day-time data are more challenging because of the need to model diurnal thermoclines. This study has highlighted the uncertainty associated with model predictions of diurnal SST changes, resulting mainly from inaccuracies in NWP flux data. Model predictions are not therefore used as a skin-to-bulk SST correction (as in the case of the skin effect), but rather to identify affected observations, which would be discarded from any further analysis. Validation using buoymatchups in section 5.2 showed a marginal improvement when this strategy was adopted.

The GODAE High-resolution SST pilot project, on the WWW at http://www.ghrsst-pp.org/

There are, however, at least two immediate problems with this approach. Firstly, there will be some areas of the oceans, such as the Mediterranean or the West Pacific, where the persistence of diurnal warming may result in very few daytime data ever being used in an analysis. Secondly, there will be some areas where diurnal warming has in reality affected observations, but these observations fail to be identified because the flux fields used in the model are deficient, and so "biased" data are subsequently included in analysis.

Improvements in the prediction of diurnal warming for AATSR processing will depend upon the availability of improved surface flux data. Validation of a Met Office NWP model air-sea flux climatology since the incorporation of humidities from satellite sounding is generally encouraging (McCulloch and Hines, 2003). In particular, the assimilation of satellite-based retrievals of wind speed (from SSM/I since Autumn 1999 and Scat since 1996) have improved the accuracy of the NWP wind field since the generation of the data used in Section 4. However, it would be worthwhile to investigate alternatives: flux climatologies based on in situ observations (Josey et al 1998; Grist and Josey 2003) or satellite-derived flux estimates may provide similar results to NWP analysis fields, and might be better validated and more reliable.

Since the quality of the flux data is the limiting factor, a sophisticated and computationally expensive physical model may be unnecessary, at least until significant improvement in flux fields has been proved. We currently use the KC model in operational AATSR processing, but it may be profitable to investigate further either a simpler physical model, or an empirical regression scheme tuned appropriately. One upper ocean model that has been used widely in the context of diurnal processes is that of Price et al. (PWP, 1986) . Two relevant studies are those of Fairall et al. (1996) and Tanahashi et al. (2003) who showed how a simplified version of the PWP model provided good results in the West Pacific against in situ and satellite observations, respectively. There are now a number of empirical regression schemes in the literature: Kawai and Kawamura (2002) and Gentemann et al. (2003) have been mentioned above; Webster et al (1996) provided a regression based on their predictions using the KC model. Future research to compare the results from a well-tuned regression scheme in AATSR diurnal thermocline predictions with results from the existing system using the KC model would be instructive. It may be that for the current purpose of identifying potentially affected AATSR data, a computationally cheap regression scheme is as effective as the detailed diurnal warming model.

Finally, in light of this study, it is clear that shallow diurnal warming should be considered not only in the case of satellite data, but also for in situ measurements of SST. In situ measurements at different depths can be biased relative to each other as a result of diurnal thermoclines: this may have an impact in the construction of climate SST analyses.

Acknowledgements

We are grateful to A. Stuart-Menteth at Southampton Oceanography Centre for provision of AVHRR Pathfinder diurnal warming data. AATSR data are © ESA and were provided within the framework of ENVISAT cal/val activities. Gary Wick at NOAA provided the original code implementation of the KC model. We thank A. O'Carroll for indispensable help in processing AVHRR and AATSR case studies. The cruise data in Figure 1 were collected as part of the ATSR PLS program and were kindly provided by T. Nightingale at Rutherford Appleton Laboratory. We also wish to thank colleagues at the Met Office and at SOC for useful discussions throughout this study.

Price-Weller-Pinkel (PWP) model available from http://www.whoi.edu/science/PO/people/jprice/

References

Candy, B., and Horrocks, L.A. Specification for a buoy/satellite matchup database for the ATSR series of radiometers. *AATSR Science Document* No. 2, Met Office, 2002.

Fairall C. W., Bradley E. F., Godfrey J. S., Wick G. A., Edson J. B., and Young G. S. Cool-skin and warm-layer effects on sea surface temperature. *J. Geophys. Res*. Vol. 101 (C1), 1295–1308, 1996.

Gentemann C. L., Donlon C. J., Stuart-Menteth A., and Wentz F. J. Diurnal signals in satellite sea surface temperature measurements. *Geophys. Res. Lett.*, Vol. 30, 1140, doi:10.1029/2002GL016291, 2003.

Gleckler P. J., and Weare B. C. Uncertainties in global ocean surface heat flux climatologies derived from ship observations. *J. Clim*, Vol. 10, 2765-2781, 1996.

Grist J. P., and Josey S. A. Inverse analysis and adjustment of the SOC air-sea heat flux climatology using ocean heat transport calculations. Submitted to *J. Clim.*, 2003.

Horrocks, L.A., O'Carroll, A.G., Saunders, R.W., Candy, B., and Harris, A.R. Near-real time processing of data from the Advanced Along-Track Scanning Radiometer (AATSR) to provide bulk sea surface temperatures. *AATSR Science Document* No. 1, Met Office, 2002.

Horrocks L. A., Candy B., Nightingale T. J., Saunders R. W., O'Carroll A., and Harris A. R. Parameterisations of the ocean skin effect and implications for satellite-based measurement of sea-surface temperature. *J. Geophys. Res.*, Vol. 108(C3), 3096, doi:10.1029/2002JC001503, 2003a.

Horrocks L. A., Saunders R. W., and O'Carroll A. An error budget for bulk sea-surface temperatures derived from AATSR data. *NWP Technical Report* No. 433, Met Office, 2003b.

Josey S. A., Kent E. C, and Taylor P. K. The Southampton Oceanography Centre (SOC) ocean-atmosphere heat, momentum and freshwater flux atlas. *Southampton Oceanography Centre Report*, No. 6, 1998.

Kantha L.H., and Clayson C.A. An improved mixed layer model for geophysical applications. *J. Geophys. Res.* Vol. 99 (C12), 25235–25266, 1994.

Kawai Y., and Kawamura H. Evaluation of the diurnal warming of sea surface temperature using satellite-derived marine meteorological data. *J. Oceanogr.* Vol. 58, 805–814, 2002.

Kraus E.B., and Turner J.S. A one-dimensional model of the seasonal thermocline II. The general theory and its consequences. *Tellus* Vol. 19, 98–105, 1967.

Large W. G., McWilliams J. C., and Doney S. Oceanic vertical mixing: A review and a model with a nonlocal boundary layer parameterization. *Rev. Geophys.* Vol. 32, 363–363, 1994.

McCulloch M. E., and Hines A. Comparison of Met Office air-sea heat fluxes with the SOC flux climatology. *Ocean Applications Technical Note* No. 31, Met Office, 2003.

Mellor G. L., and Yamada T. Development of a turbulent closure model for geophysical fluid problems. *Rev. Geophys. Space Phys.* Vol. 20, 851–875, 1982.

Morel A., and Antoine D. heating rate within the upper ocean in relation to its bio-optical state. *J. Phys. Oceanogr.* Vol. 24, 1652–1665, 1994.

Paulson C. A., and Simpson J. J., Irradiance measurements in the upper ocean. *J. Phys. Oceanogr.* Vol. 7, 952–956, 1977.

Price J. F., Weller R. A., and Pinkel R. Diurnal cycling: Observations and models of the upper ocean response to diurnal heating, cooling and wind mixing. *J. Geophys. Res.* Vol. 91, 8411–8427, 1986.

Simpson J. J., and Dickey T. D. The relationship between downward irradiance and upper ocean structure. *J. Phys. Oceanogr.* Vol. 11, 309–323, 1981.

Stuart-Menteth A. C., Robinson I. S., and Challenor, P. G. A global study of diurnal warming using satellite-derived sea surface temperature. *J. Geophys. Res.* Vol. 108(C5), 3155, doi: 10.1029/2002JC001534, 2003.

Tanahashi S., Kawamura H., Takahashi T., and Yusa H. Diurnal variations of sea surface temperature over the wide-ranging ocean using VISSR on board GMS. *J. Geophys. Res.* Vol. 108(C7), 3216, doi: 10.1029/2002JC001313, 2003.

Webster P.J., Clayson C.A., and Curry J.A. Clouds, radiation, and the diurnal cycle of SST in the tropical Western Pacific. *J. Clim.* Vol. 9**,** 1712–1730, 1996.

Wick G.A. Evaluation of the variability and predictability of the bulk-skin sea surface temperature difference with application to satellite-measured sea surface temperature. *PhD Thesis,* U. Colorado (Boulder), 1995.

Figures

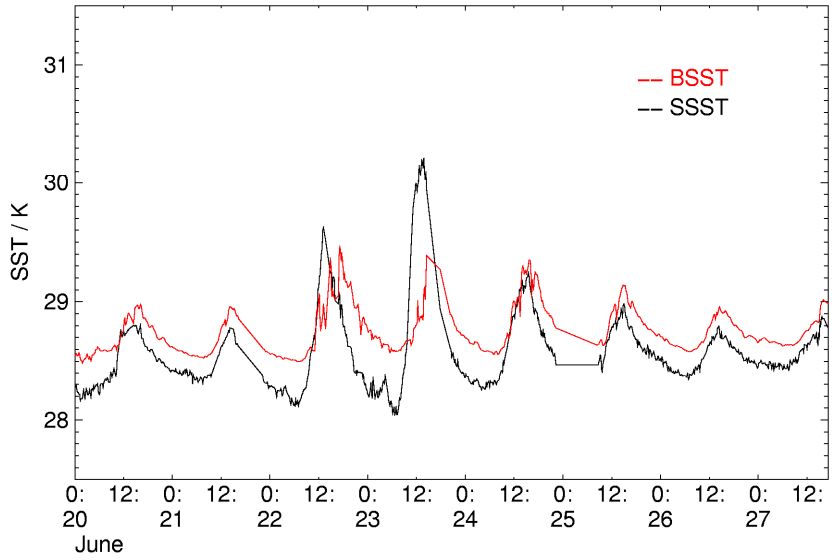

Figure 1. Measurements of bulk SST at 4.5 m (red line) and infrared skin SST (black line) taken from a cruise in the western Pacific during 1999. Infrared skin SST is usually cooler than the bulk SST. In the afternoon of 22 and 23 June, the skin SST becomes warmer than bulk SST, indicating stably stratified surface waters, the result of shallow warming from insolation (a diurnal thermocline). Data courtesy of T. Nightingale, R.A.L.

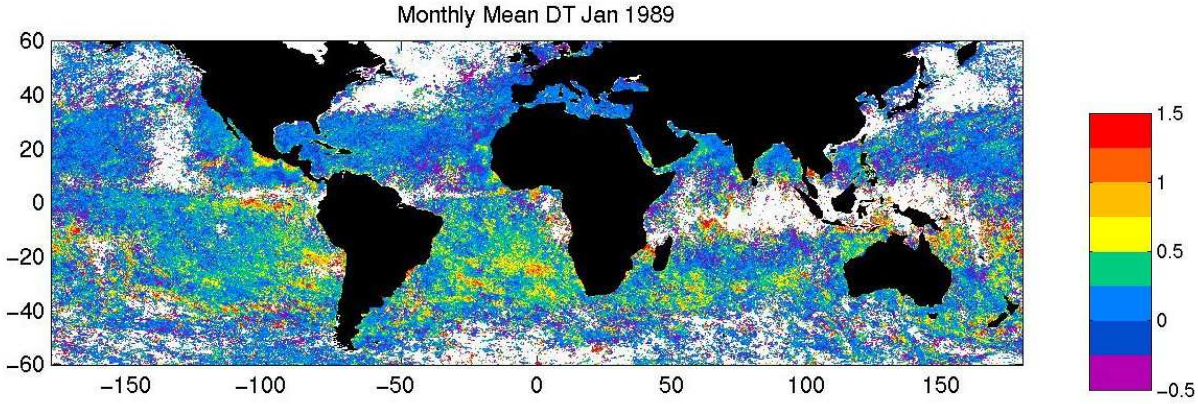

Figure 2. Observed day–night SST differences from AVHRR data during January 1989. AVHRR has a wider swath than (A)ATSR and differences between consecutive day and night SSTs can be computed. The afternoon overpass in mid-afternoon is close to the peak of the diurnal cycle. (Figure courtesy of A. Stuart-Menteth, SOC).

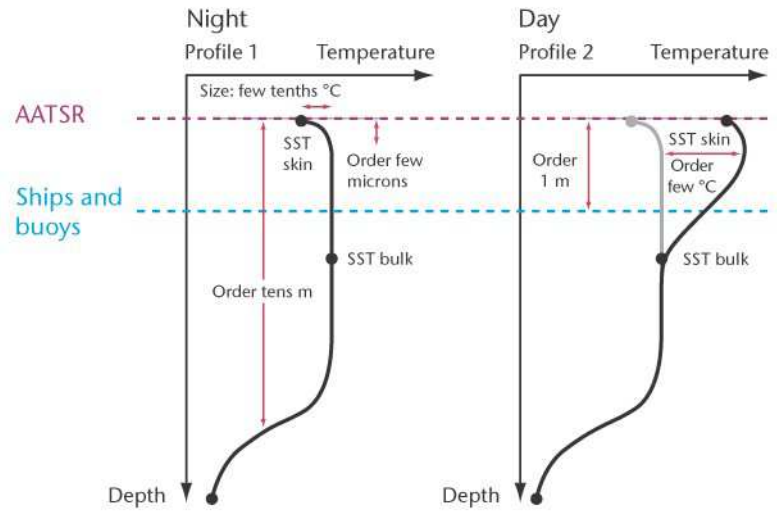

Figure 3. Schematic temperature profiles at the ocean surface for night, or cloudy, windy conditions (Profile 1) and calm clear daytime (Profile 2).

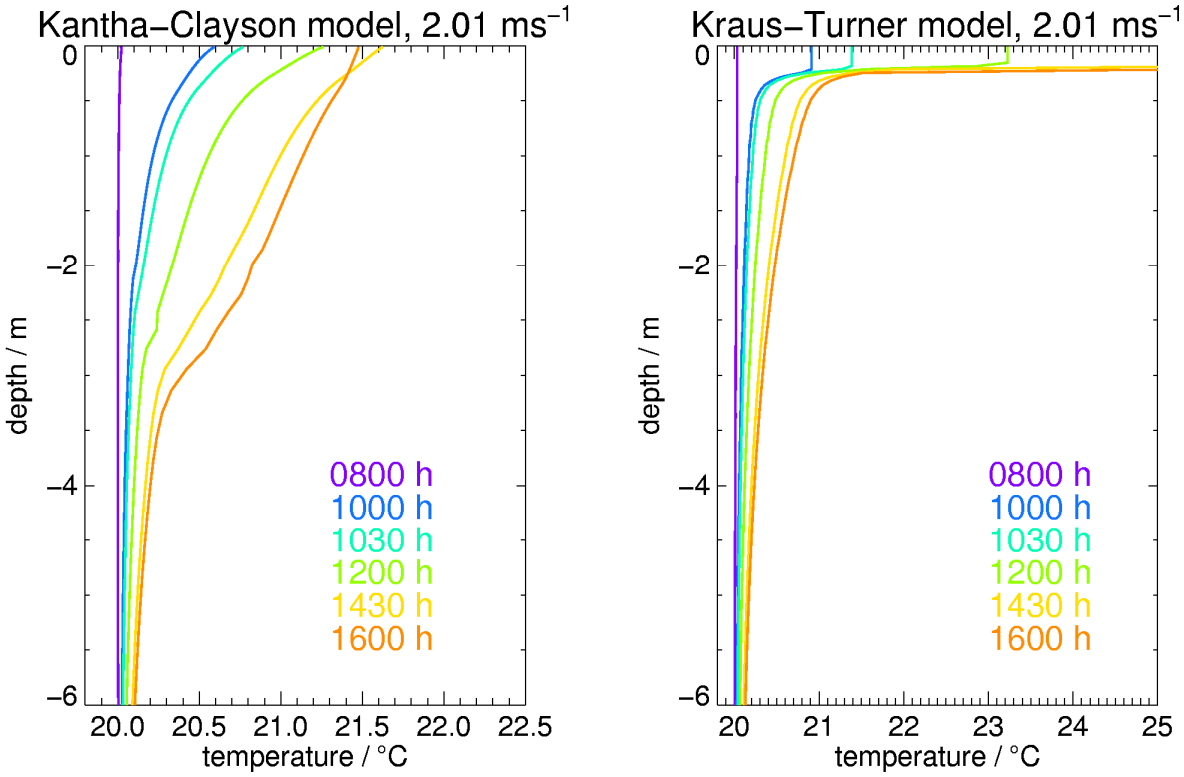

Figure 4. Simulations of shallow diurnal warming using KC and KT models, running from dawn at 0600 h through to the times indicated on the figure. Wind speed was assumed constant at ~2.0 ms^{-1}. Peak solar flux was 1000 Wm^{-2} occurring at 1200 h, latent heat flux was 75 Wm^{-2}, and total non-solar fluxes were 150 Wm^{-2}. Note the different scales on the temperature axes. Daylight overpass times for ATSR-1 and -2 are ~1030 h local time, for AATSR ~1000 h. The NOAA series satellites (with AVHRR) have generally had daylight overpass times during local afternoon.

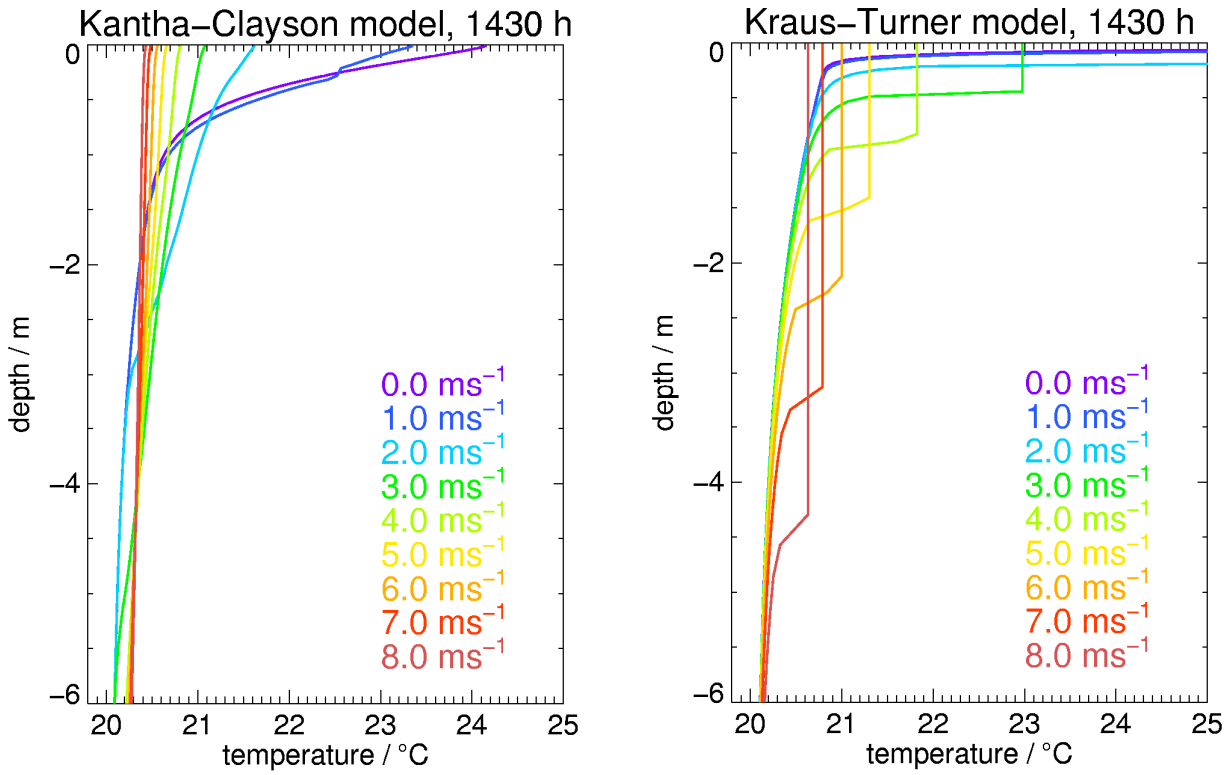

Figure 5. Simulations of shallow diurnal warming from KC and KT models by 1430 h (assuming dawn at 0600h). Heat fluxes were the same as for Figure 4. Coloured curves illustrate results for different fixed wind speeds, as shown.

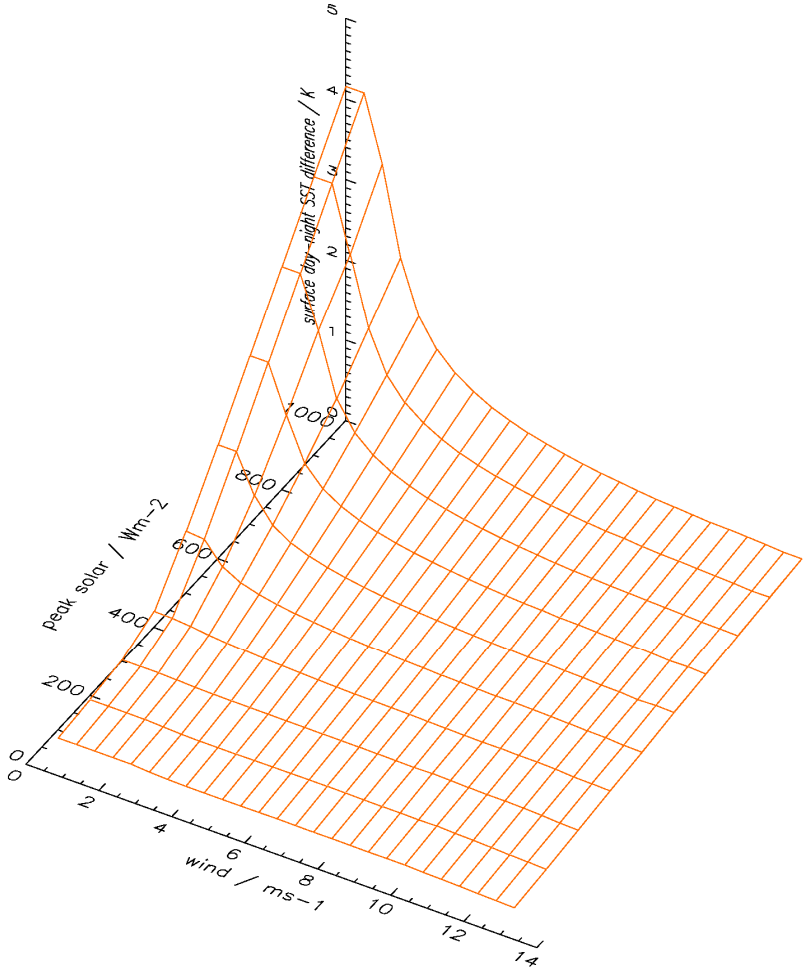

Figure 6. Simulations using the KC model for a range of wind speeds and peak solar radiation fluxes. Other heat fluxes were the same as for Figure 4, and the model was run through to 1430 h. The surface layer temperature increase between initialisation and 1430 h is shown on the z-axis.

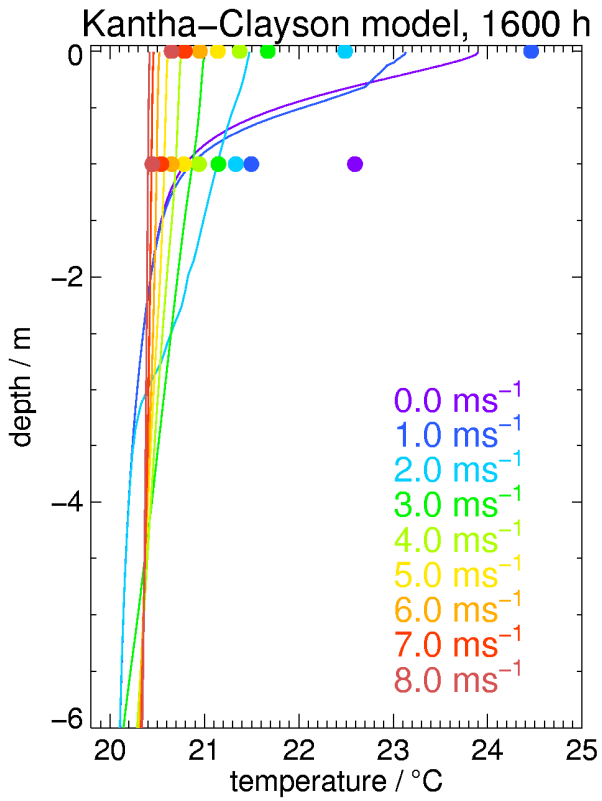

Figure 7. Profiles for KC model at 1600 h, plotted as in Figure 5. Dots indicate predicted maximum diurnal temperature excursions at skin and 1-m depth from the regression scheme of Kawai and Kawamura (2002), colours correspond to wind speed. The dot representing predicted surface temperature excursion at 0.0 ms^{-1} is off the scale. The same flux data were used for both models.

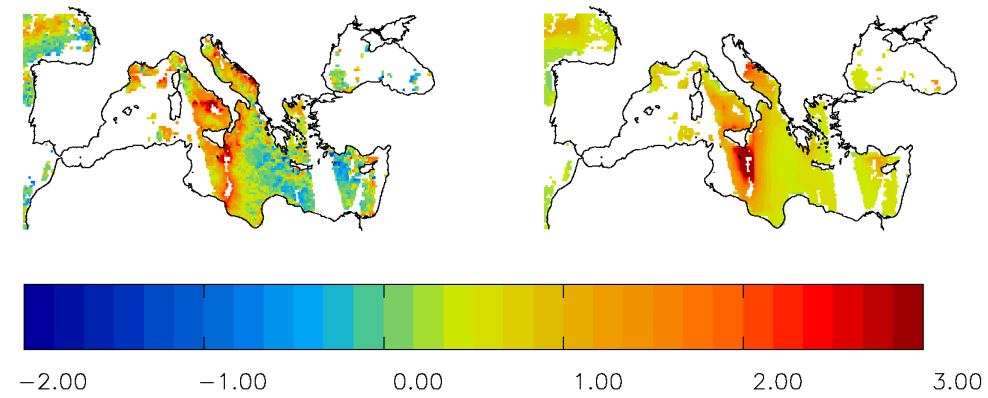

Figure 8. Measured (left) and predicted (right) day–night SST difference on 14 July 1997. Measurements were computed from AVHRR SST retrievals. Predictions were determined using KC model and Met Office NWP flux data. Data gaps result from cloud detection and/or no day/night overlap of overpasses. See text for details. Key bar marked in K.

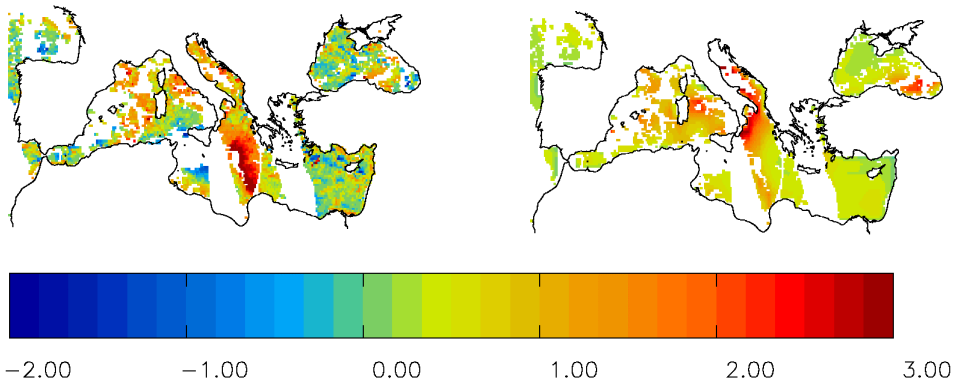

Figure 9. Measured (left) and predicted (right) day–night SST difference on 10 July 1997. (As Figure 8.)

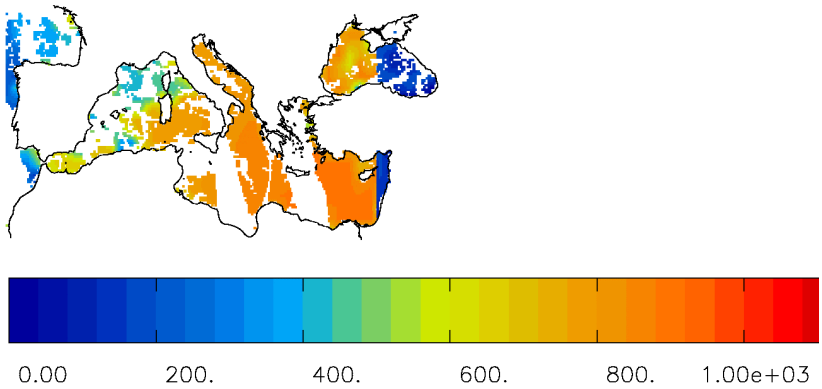

Figure 10. NWP analysis 6-hour mean solar flux during morning prior to AVHRR overpasses on 10 July 1997. Note that there is no evidence for cloud in the central Mediterranean where strong diurnal warming is seen in Figure 9. The sharp change at far east of plot occurs because overpasses here are matched up with NWP model data of the previous 6-hour analysis. Key bar marked in Wm^{-2}.

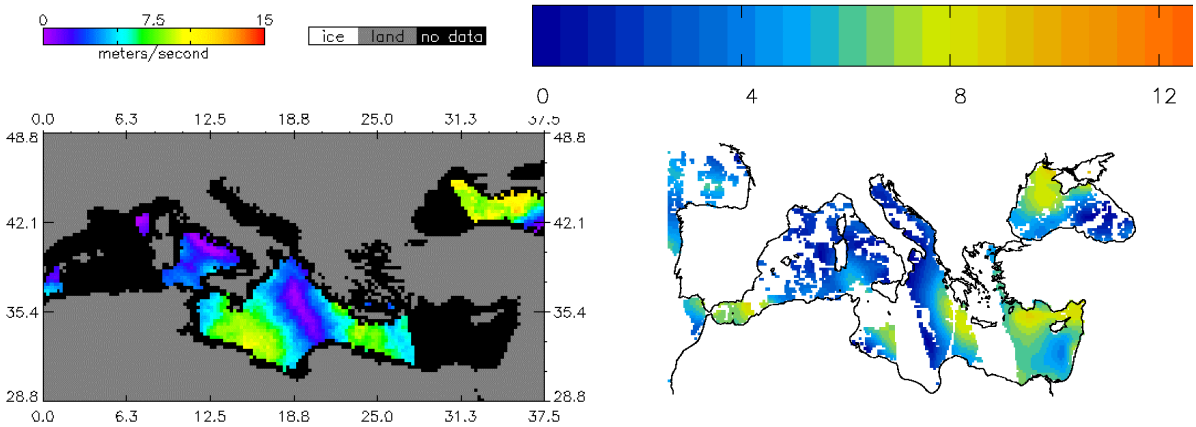

Figure 11. Wind speed on 10 July 1997. Observations from SSM/I (left, with scale above), and Met Office NWP model analysis (right, with scale above). Note that the region of ~0 ms^{-1} wind speed identified in the observations correlates with the region of diurnal warming observed from AVHRR (Figure 9), but the NWP analysis does not locate this area entirely accurately.

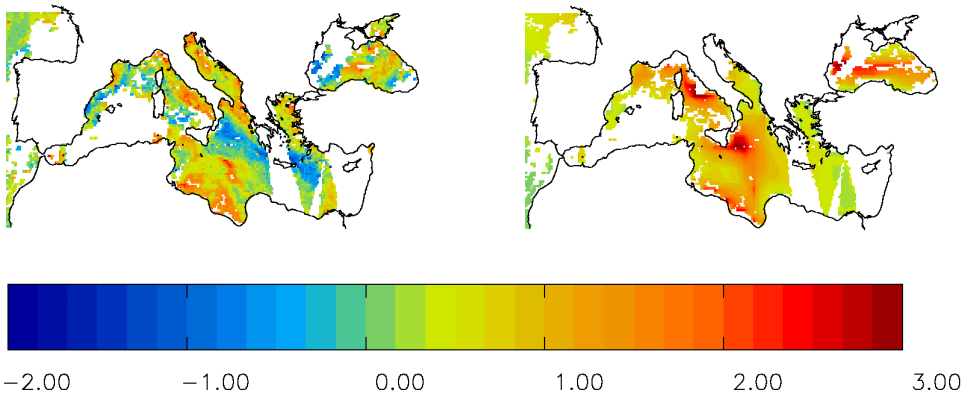

Figure 12. Measured (left) and predicted (right) day–night SST difference on 22 July 1997. Note the large area of apparent diurnal cooling in the AVHRR measurements.

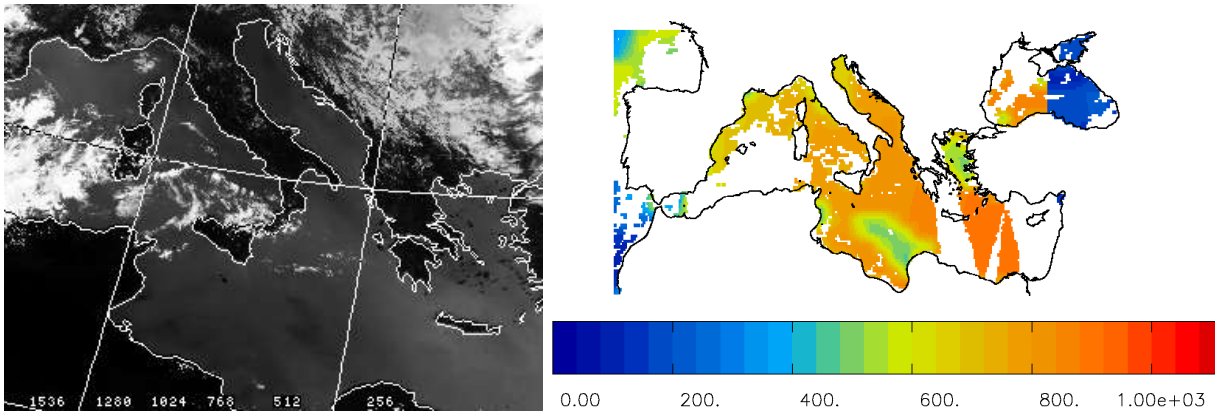

Figure 13. AVHRR Channel 4 imagery for daytime on 22 July 1997 (left) shows thin cloud stretching ESE from Sicily. The NWP model solar flux field indicates cloud present in the analysis, but misplaced too far south.

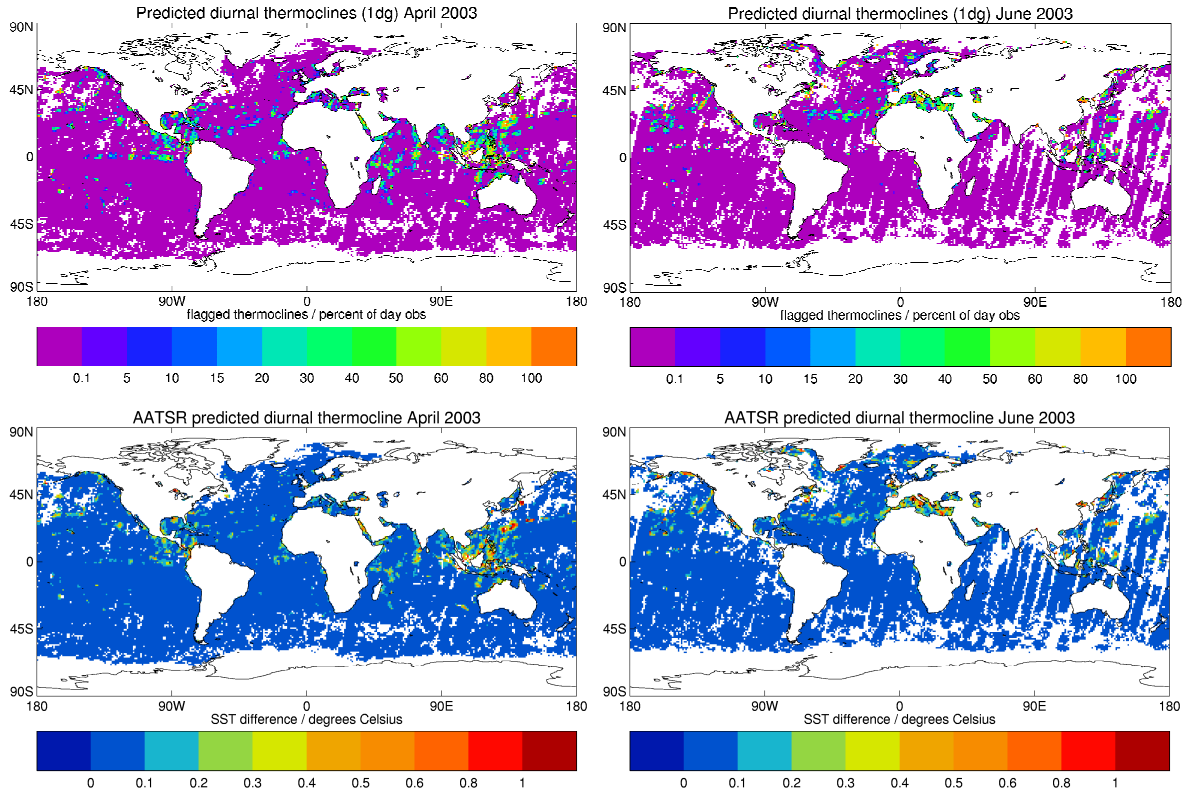

Figure 14. Upper: Frequency of predicted diurnal thermoclines in daytime AATSR observations for April (left) and June 2003; diurnal thermoclines were flagged when the predicted skin–1-m SST difference was more than 0.2 K. Lower: Average predicted skin–1-m SST difference for the same months. The data gaps in the June plot are the result of unavailability of NWP flux data within the timeframe of near-real time processing.